Acta Chemica Scandinavica, 1999: 53: 920–927
Printed in UK. All rights reserved

ACTA
CHEMICA SCANDINAVICA
ISSN 0904-213X

Reactivity of Transient 17- and 19-Electron Nickel(I)-Centred Radicals: $CpNi(PR_3)$ and $CpNi(PR_3)_2$. Redox Properties and Formation of the Zero-Valent Anionic Nickelate $CpNi(PPh_3)^-$

Christian Amatore,* Olivier Buriez and Jean-Noël Verpeaux

Département de Chimie de l'Ecole Normale Supérieure, UMR 8640, 24 rue Lhomond, F 75231 Paris Cedex 05, France

Dedicated to Professor Henning Lund on the occasion of his 70th birthday.

Amatore, C., Buriez, O. and Verpeaux, J.-N., 1999. Reactivity of Transient 17- and 19-Electron Nickel(I)-Centred Radicals: $CpNi(PR_3)$ and $CpNi(PR_3)_2$. Redox Properties and Formation of the Zero-Valent Anionic Nickelate $CpNi(PPh_3)^-$. *Acta Chem. Scand.* 53: 920–927. © Acta Chemica Scandinavica 1999.

The electrochemical reduction of $CpNi(PR_3)_2^+$, BF_4^- and $Cp(PR_3)NiCl$ (R = Bu or Ph) complexes in THF or acetonitrile has been investigated in order to characterize the transient paramagnetic Ni^I species. Indeed, on the short timescale of cyclic voltammetry, the reduction of both complexes leads to the 17-electron monophosphine compound, through a reversible decoordination of one phosphine in the first case, and directly in the second case; this radical rapidly evolves to form nickelocene, but its further reduction yields the corresponding nickelate $Cp(PR_3)Ni^- Bu_4N^+$ which could be trapped by a tin electrophile.

Electron transfer to transition metal centered compounds leads, in most cases, to substantial activation of the coordination shell; a relaxation process ensues[1–3] which may correspond to an isomerization, a change of hapticity, or the fixation of an extra ligand, an insertion or migration process, the cleavage of a frangible bond, etc. In organometallic chemistry, transient paramagnetic 17- or 19-electron complexes[4–6] are generally formed directly by the addition or uptake of one electron to or from the starting 18- (sometimes 16-) electron substrate, but also as primary products of one of the above-mentioned reactions, which essentially imply an even number of electrons.

In the course of our research program concerning the electron transfer activation of selected σ-alkyl transition metal complexes, we turned our attention to nickel derivatives in the Cp(L)NiR series,[7] where L is a phosphine and R represents various alkyl groups of interest. However, to perform this investigation, and be able to decipher the voltammetric patterns and extract the mechanistic scheme of this rich and versatile electrochemistry, it rapidly turned out that it was essential to gain, as a prerequisite, some knowledge about the chemistry and electrochemistry of the Ni^I fragment CpNi(L) expected to be formed at some stage of the reductive activation of Cp(L)NiR.

Very little information could be obtained from the literature concerning this highly unstable 17-electron nickel(I) species, since in a general way, the chemistry of nickel(I) is very poorly described.[8] Although not directly observed, $CpNi(PPh_3)$ has been proposed as the product of further evolution of the 19-electron $CpNi(PPh_3)_2$ generated by electrochemical reduction of the corresponding cation in acetonitrile.[9] Indeed, in the early eighties, several groups[9–11] studied the electroreduction of $CpNi(PR_3)_2^+$ in classical electrochemical media (acetonitrile, DMF, dichloromethane). Their results can be summarized as follows: on the timescale of cyclic voltammetry, the 19-electron neutral complex is fully stable when PR_3 is a trialkylphosphine, but only partially with triphenylphosphine; in the latter case, an increase of reversibility was observed when the voltammogram was run in the presence of free triphenylphosphine, which was the indication of the formation of $CpNi(PPh_3)$. No other information on this 17-electron compound was available since on the longer timescale of preparative electrolysis, only nickelocene and $Ni(PR_3)_n$ were recovered. We therefore decided to reinvestigate the electro-

* To whom correspondence should be addressed.

chemical reduction of $Cp(PR_3)_2Ni^+$ in a broader potential range, on different timescales, and to compare it with the as yet unreported voltammetry of $Cp(PR_3)NiCl$, which was expected to lead to the same 17-electron intermediate after reduction and loss of a chloride ion. For compliance with our more general organometallic study, THF was chosen as the solvent but acetonitrile was also used since preliminary studies[9–11] had utilised it.

Results

Electrochemical reduction of $CpNi(PR_3)_2^+ BF_4^-$. The cyclic voltammograms obtained by reduction of $CpNi(PR_3)_2^+ BF_4^-$ (R = Bu, Fig. 1 or Ph, Fig. 2) in THF or acetonitrile at 0.5 V s^{-1} and room temperature show a partially chemically reversible wave R_1. In the same solvent, the reduction potential of a cationic nickel(II) salt is about 300 mV more positive for the triphenylphosphine derivative than for the tributylphosphine analogue, in agreement with the stronger electron donating properties of the latter. For the same compound the reduction potential is shifted toward more positive values when acetonitrile is replaced by THF, as is expected from the better solvation and stabilisation of the cationic form in the former solvent.

At 0.5 V s^{-1} this wave R_1 has a peak-to-peak separation of 60 mV in acetonitrile, in agreement with a Nernstian electron transfer, and in the range 80–90 mV in THF, also suggesting Nernstian behaviour since the ferrocene–ferricinium couple led to the same value in this rather resistive solvent at the same electrode and potential scan rate. As already mentioned, the reversibility is more pronounced and in fact nearly complete for the compound bearing a trialkylphosphine ligand; compare Figs. 1a and 2a. Table 1 gives the standard potentials E° and the ratio of anodic to cathodic peak current at 0.5 V s^{-1} for these two compounds in the two solvents.

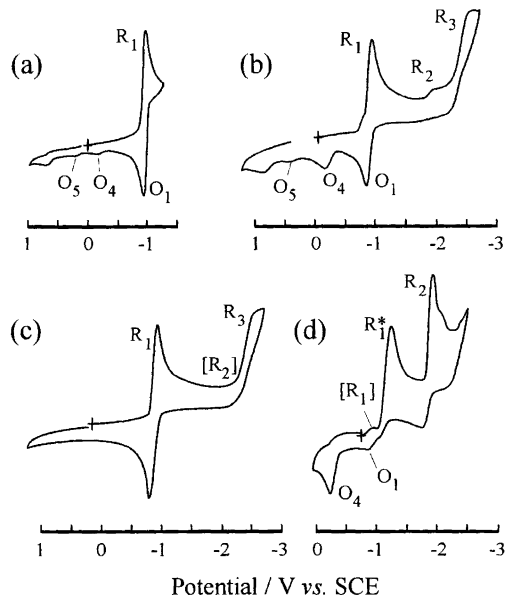

Fig. 1. Cyclic voltammetry at 0.5 V s^{-1} of $CpNi(PBu_3)_2^+ BF_4^-$ (2 mM) in THF–NBu_4BF_4 0.3 M at room temperature on a 0.5 mm diameter gold disc electrode: (a) and (b) complex alone; (c) in the presence of two molar equivalents of PBu_3; (d) cyclic voltammetry of $Cp(PBu_3)NiCl$ under the same conditions as (b). The disappearance of wave R_2 in (c) is denoted by the symbol $[R_2]$; the small wave R_1 in (d) seems to be due to a tiny amount of $[CpNi(PBu_3)THF]^+$, see Ref. 13.

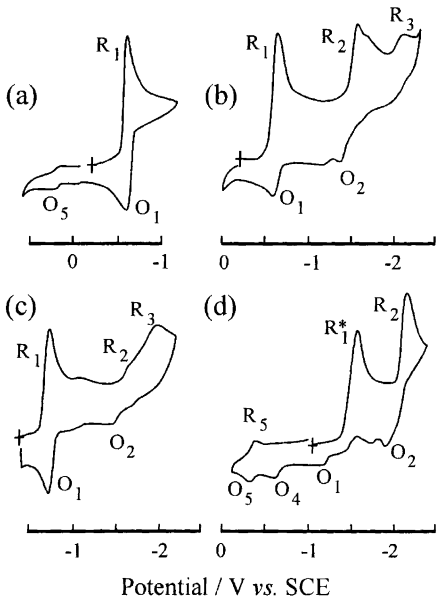

Fig. 2. Cyclic voltammetry at 0.5 V s^{-1} of $CpNi(PPh_3)_2^+ BF_4^-$ (2 mM) in THF–NBu_4BF_4 0.3 M at room temperature on a 0.5 mm diameter gold disc electrode: (a) and (b) complex alone; (c) in the presence of one molar equivalent of PBu_3; (d) cyclic voltammetry of $Cp(PPh_3)NiCl$ under the same conditions as (b).

The degree of reversibility of the reduction wave of $CpNi(PPh_3)_2^+$ depends on the potential scan rate, although in a non-monotonous way: in THF, it was found to reach a minimum value ($i_a^p/i_c^p \approx 0.45$) for a potential scan rate of 2 V s^{-1}. This result was confirmed by double step chronoamperometry since the ratio of the backward to the forward diffusion current also had a minimum value corresponding to a step duration of 20 ms.

Extension of the potential scan to more negative values revealed two additional reduction waves, R_2 and R_3 in THF; in acetonitrile where the intrinsic discharge of the solvent happens earlier, only R_2 is visible. For the tributylphosphine complex, R_2 is rather small compared

Table 1 Standard potentials in V vs. SCE and anodic-to-cathodic peak current ratio at 0.5 V s^{-1} for the $CpNi(PR_3)_2/CpNi(PR_3)_2^+$ redox couples.

	$CpNi(PPh_3)_2^+$		$CpNi(PPh_3)_2^+$	
Solvent	E°/V	(i_a^p/i_c^p)	E°/V	(i_a^p/i_c^p)
Acetonitrile	−0.83	(0.75)	−1.15	(1)
THF	−0.65	(0.6)	−0.95	(0.9)

with R_1 and R_3 (see Fig. 1b), whereas for the triphenylphosphine analogue, it is more prominent (Fig. 2b). In both cases, the size of R_2 decreases with increasing potential scan rate; conversely, the size of R_3 remains approximately constant with the scan rate in THF.

The backward potential scan shows two small and sometimes ill-defined oxidation waves (denoted O_4 and O_5 in the following), in addition to the oxidation wave O_1 corresponding to the reversibility of wave R_1. All these oxidation or reduction peak potentials are collected in Table 2. In each solvent, O_5 could easily be assigned to the first oxidation of nickelocene, the ultimate product of the reduction,[9-11] by comparison with the behaviour of an authentic sample.

When the voltammograms were run in the presence of added free phosphine, see Figs. 1c and 2c, several modifications were observed: (*i*) wave R_1 appeared much more reversible (PPh_3); (*ii*) wave R_2 disappeared but wave R_3 remained unchanged (PBu_3) or increased (PPh_3). This shows that adding free phosphine has a similar effect as increasing the potential scan rate on the reductive pattern of $CpNi(PR_3)_2^+$.

Electrochemical reduction of $CpNi(PR_3)Cl$. The cyclic voltammograms obtained from the nickel chloride complexes $CpNi(PR_3)Cl$ show a first reduction wave R_1* (see Figs. 1d and 2d), which remains chemically irreversible even at several thousands volts per second. As expected, the reduction potential is more negative than that of the corresponding bis-phosphine cation in the same solvent (Table 2). The method[12] combining chronamperometry and steady-state voltammetry to determine both the absolute number of electrons *n* involved in an irreversible wave and the diffusion coefficient of the species was applied to the reduction of $CpNi(PBu_3)Cl$ in THF; it unambiguously established that wave R_1* is monoelectronic ($n = 1$). The same measurement could not be performed in the case of $CpNi(PPh_3)Cl$ because of poor reproducibility of the steady-state current at the 25 μm diameter microelectrode, probably due to fouling by triphenylphosphine. However, the sizes of the waves obtained from $CpNi(PPh_3)Cl$ and $CpNi(PBu_3)Cl$ under the same conditions are practically identical. This shows that the reduction of the triphenylphosphine complex is also monoelectronic, since the diffusion coefficients (acting as their square root) cannot possibly be so different as to compensate a modification of *n* from 1 to another value such as 0.5, 2 or even 1.5.

Table 2 Peak potentials E^p (in V vs. SCE) measured at 0.5 V s^{-1}, in THF or acetonitrile (ACN) for reduction and oxidation waves displayed after initial reduction of $CpNi(PR_3)_2^+$ (wave R_1) or $CpNi(PR_3)Cl$ (wave R_1*).

		R = Ph		R = Bu	
Wave	Assignment	in THF	in ACN	in THF	in ACN
R_1	$CpNi(PR_3)_2^+$	−0.70	−0.86	−1.00	−1.18
R_1*	$CpNi(PR_3)Cl$	−1.01	−1.01[a]	−1.30	−1.30[a]
R_2	$CpNi(PR_3)$	−1.63	−1.63	−1.93	−1.93
R_3	$CpNi(PR_3)_2$	−2.10		−2.50	
O_1	$CpNi(PR_3)_2$	−0.60	−0.80	−0.90	−1.12
O_4	$CpNi(PR_3)$	−0.02	−0.30	−0.27	−0.43
O_5	Cp_2Ni	0.20		0.20	0.06

[a] This reduction wave is preceeded by a small and ill-defined wave that could be assigned to the reduction of $[Cp(PR_3)Ni(ACN)]^+$ formed by a dynamic shift of a reversible displacement of Cl by the solvent according to a CE mechanism.[13]

In all cases, this reduction wave R_1* is followed by a second one, R_2 located at the same potential but significantly bigger than the second wave issuing from the reduction of $CpNi(PR_3)_2^+$; this is apparent in Figs. 1d and 2d. Actually, the size of wave R_2 appears very similar to the size of R_1* suggesting that the same number of electrons is involved in these two reduction stages. This also could be confirmed by using both steady-state voltammetry at a small microelectrode and very low potential scan rate, and chronoamperometry with duration steps varying from 5 to 500 ms, where the step potential is fixed after R_1* for the first measurement and after R_2 for the second. Indeed, these two techniques give better quantitative results than cyclic voltammetry since the measurements of plateau values are more accurate and also because the plateau current (in steady-state voltammetry) or diffusion current (in chronoamperometry) are independent of the electrochemical mechanism for the same number of electrons exchanged.[14,15]

The reduction of $Cp(PBu_3)NiCl$ in THF generates one compound whose oxidation wave (Fig. 1d) is located at the same potential as the wave O_4 observed from the cationic bis-phosphine complex; the size of O_4 is now bigger, as it was for wave R_2. Double step chronoamperometry (first step on the plateau of R_1* immediately followed by a second step of the same duration on the plateau of O_4) indicates a yield in the region of 75% for this product. In the case of $Cp(PPh_3)NiCl$, (Fig. 2d) the two waves O_4 and O_5 (nickelocene) are observed on the reverse potential scan.

Reduction in the presence of added electrophile. The possibility of trapping a reduced nickel intermediate by adding an electrophile was then studied. The addition of hydroquinone as a proton donor, to the solution of nickel complexes gave encouraging results: the position and the size of waves R_1, R_1*, R_2 or O_4 were not significantly altered, but the partial reversibility of wave R_2 (see Figs. 2b and 2d, see also Fig. 3a) was completely erased. Moreover, a new reduction wave was visible, although small and partially overlapping with background discharge current; the fact that the new wave appears around −2.15 V with $Cp(PPh_3)NiCl$ or $Cp(PPh_3)_2Ni^+$ solutions and around −2.5 V with $Cp(PBu_3)NiCl$ excludes the hypothesis of a reduction of the proton of hydroquinone and suggests the reduction of a protonated species.

More definitive conclusions could be drawn with

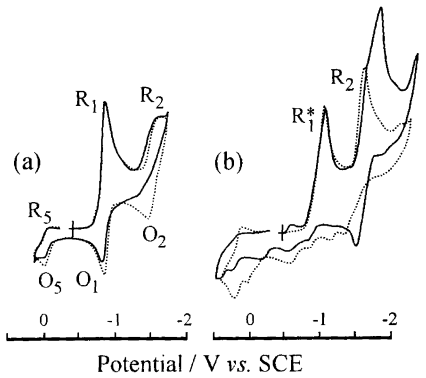

Fig. 3. (a) Cyclic voltammetry at 0.5 V s^{-1} of $CpNi(PPh_3)_2^+$ BF_4^- (2 mM) in acetonitrile–NBu_4BF_4 0.3 M at room temperature on a 0.5 mm diameter gold disc electrode in the presence (full line) and absence (dotted line) of hydroquinone (4 mM); (b) cyclic voltammetry at 0.5 V s^{-1} of $Cp(PPh_3)NiCl$ (2 mM) in THF–NBu_4BF_4 0.3 M at room temperature on a 0.5 mm diameter gold disc electrode in the presence (full line) and absence (dotted line) of Ph_3SnCl (2 mM).

triphenyltin chloride; indeed, when one molar equivalent of this electrophile was added to the solution of $Cp(PPh_3)NiCl$ in THF, a new reduction wave clearly appeared just behind wave R_2 with partial overlap, see Fig. 3b. This wave is chemically reversible, with a standard potential of -1.71 V and could be assigned to the reversible reduction of $Cp(PPh_3)NiSnPh_3$ by comparison with the electrochemical behaviour of a sample independently prepared[16] by reaction of Ph_3SnLi with $Cp(PPh_3)NiCl$. It should also be noted (Fig. 3b) that the presence of the tin electrophile significantly decreases the size of wave O_5.

A very similar experiment, with tributyltin chloride used in place of triphenyltin chloride gave rise to a related chemically reversible reduction wave at $E^\circ = -1.95$ V. The negative shift observed for the standard redox potential is easily explained by the structural modification from $Cp(PPh_3)NiSnPh_3$ to $Cp(PPh_3)NiSnBu_3$.

Preparative scale reduction of $Cp(PPh_3)NiCl$. The electrolysis of an 87 mM solution of $Cp(PPh_3)NiCl$ in a 0.1 M solution of *n*-Bu_4N BF_4 in acetonitrile was performed at a controlled potential of -1.0 V corresponding to wave R_1* and, in a second experiment, at -1.65 V, i.e. at the potential of R_2. Rigorously identical results were obtained in both electrolyses: (*i*) the complete consumption of the starting nickel chloride required less than one faraday (approximately 0.6 F), showing that the electron stoichiometry differs from the one electron per mole at wave R_1* and one electron more at wave R_2 measured by voltammetry, and (*ii*) the formation of nickelocene in a nearly quantitative yield (with respect to Cp) as the only product visible on the cyclic voltammogram of the reaction mixture at the end of the electrolysis.

Several electrolyses were performed at the potential of wave R_2 in the presence of a tin electrophile. When an equimolar amount of Ph_3SnCl was present, the electron consumption was raised to 1.3 F. The heterobinuclear compound $Cp(PPh_3)NiSnPh_3$ was indeed formed but only as a minor product, generation of nickelocene (75%) being still the favoured process. Increasing the molar ratio of tin chloride to nickel species from 1 to 4 resulted in the consumption of 2 F, an increase of the yield of $Cp(PPh_3)NiSnPh_3$ and a related decrease of the yield of nickelocene (55%).

The reduction potential of $Cp(PPh_3)NiSnPh_3$ ($E^p = -1.79$ V) is very close to the potential of R_2 chosen for the electrolyses (-1.6 V); this could well be responsible for the poor final yield of this complex. Similar electrolyses were therefore run with Bu_3SnCl in place of Ph_3SnCl. The electron consumption was now 1 F for a molar equivalent of tin chloride and rose to 1.9 F when 4 molar equivalents were used; however the yield of nickelocene remained very high (>90%) in both experiments.

Discussion

Electrogeneration of 19- and 17-electron nickel(I) species. The reduction of the cationic $CpNi(PR_3)_2^+$ species corresponds to a Nernstian voltammetric wave, both in THF or acetonitrile and leads to the 19-electron neutral complex, eqn, (1).

$$CpNi(PR_3)_2^+ + e \rightleftharpoons CpNi(PR_3)_2 \quad (1)$$

With tributylphosphine, this paramagnetic species appears stable even on the timescale of slow cyclic voltammetry, which corresponds to a one second range. Conversely, when R is phenyl, the chemical reversibility of the reduction wave follows a non-monotonous variation with the potential, showing a minimum value around 2 V s^{-1} in THF. This is characteristic of a reversible follow-up reaction of the electrogenerated paramagnetic $CpNi(PPh_3)_2$ with a high equilibrium constant [eqn. (2)] corresponding to a right-hand side displacement. In the case at hand, both the previous studies[9–11] and the effect of added free phosphine shows that this reversible reaction is a decoordination of one phosphine ligand.

$$CpNi(PPh_3)_2^+ + e \rightleftharpoons CpNi(PPh_3)_2 \overset{k_f}{\rightleftharpoons} CpNi(PPh_3) + PPh_3 \quad (2)$$

At high potential scan rate, the forward chemical reaction (k_f) is progressively kinetically frozen and more and more $CpNi(PPh_3)_2$ remains in the diffusion layer when its oxidation potential is reached on the reverse scan; conversely at lower potential scan rate, the forward reaction has enough time to operate and the reduction of the starting cation leads, through $CpNi(PPh_3)_2$, to the monophosphine paramagnetic nickel species and free PPh_3. However, during the reverse scan and at very slow potential scan rate, the oxidation leading to consumption of $CpNi(PPh_3)_2$ at the level of wave O_1 can displace the equilibrium toward the left hand side, since at this long

timescale, k_b is operative. The minimum of reversibility observed in both cyclic voltammetry and chronoamperometry corresponds to a timescale where the forward reaction proceeds but the backward one is mostly frozen. This dynamic equilibrium also explains the fact that the reversibility is fully restored in the presence of extra phosphine.

The 19-electron $CpNi(PR_3)_2$ is more stable *vis-à-vis* the loss of one phosphine in acetonitrile than in THF, and, as already mentioned, when trialkyl- rather than triaryl-phosphines are involved. In between waves R_1 and R_2, the composition of the diffusion layer is representative of the degree of establishment of the decoordination equilibrium (nature of PR_3 and solvent, timescale) in addition to the usual diffusion factors.

When the corresponding chloride $Cp(PR_3)NiCl$ is reduced, the wave R_1* remains irreversible whatever the scan rate,[15] and quantitatively generates a species that is reduced at wave R_2. The fact that R_1* is monoelectronic, and the formation of the same product (reduced at R_2) as when starting from the diphosphine cation, clearly establishes that the cleavage of the nickel chloride bond is the first step [eqn. (3)] of the reduction process.

$$Cp(PR_3)NiCl + e \rightarrow CpNi(PR_3) + Cl^- \qquad \text{(overall}^{15}\text{ eqn. 3)}$$

It then appears that both complexes $CpNi(PR_3)_2^+$ and $Cp(PR_3)NiCl$ give, upon reduction, the same paramagnetic Ni^I complex although through a slow and reversible pathway for the former, and more directly for the latter.

This explains all the results obtained from the reduction part of the cyclic voltammograms. Indeed, if we assume that wave R_2 corresponds to the reduction of the 17-electron radical $CpNi(PR_3)$ and R_3 to the reduction of the 19-electron $CpNi(PR_3)_2$, the effects of potential scan rate, of the nature of the phosphine and of extra free phosphine on the size of these waves during the reduction of $CpNi(PR_3)_2^+$ are easily understood, since all that disfavours the formation of $CpNi(PR_3)$ from $CpNi(PR_3)_2$ (short timescale, strongly coordinating phosphine, excess of free phosphine) actually leads to a decrease of R_2 compared with R_3.

In the case of the reduction of $Cp(PR_3)NiCl$, the fast and irreversible character of the cleavage of the nickel–chlorine bond explains the one-to-one ratio of the size of waves R_1* and R_2 (and the quasi-absence of R_3) whatever the scan rate since it leads to a straightforward production of $CpNi(PR_3)$.

Assignment of wave O_4; stability of the 17-electron radical. All the voltammograms display, on their reverse oxidative scan, the wave O_4, the size of which depends on the precursor, the solvent and the potential scan rate. For instance, it is visible, although very small in Fig. 1a, and significantly developed in Fig. 1d. When cationic bis-phosphinenickel derivatives are reduced, the size of O_4 decreases with increasing scan rate or added phosphine, which shows that O_4 is associated with $CpNi(PR_3)$ rather

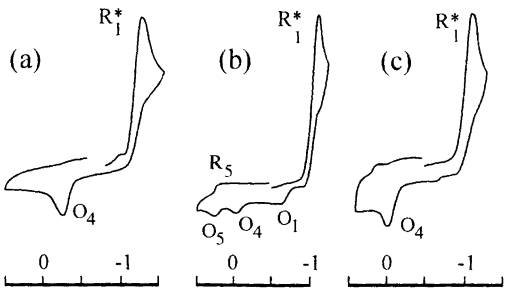

Fig. 4. Cyclic voltammetry of $Cp(PR_3)NiCl$ (2 mM) in THF–NBu_4BF_4 0.3 M at room temperature on a 0.5 mm diameter gold disc electrode: (a) at 0.5 V s^{-1}, R = Bu; (b) at 0.5 V s^{-1}, R = Ph; (c) at 20 V s^{-1}, R = Ph.

than the 19-electron bis-phosphine radical. This is clearer still from the voltammograms obtained upon reduction of the nickel chloride complexes: when $CpNi(PR_3)$ is generated by the straightforward process, O_4 is the major oxidation wave on the reverse scan (see Fig. 4) at least on a sufficiently short timescale. This correlation between the appearance and size of waves R_2 and O_4, as well as the location of these waves about 500–600 mV more positive than the oxidation waves O_1 due to the oxidation of the 19-electron $CpNi(PR_3)_2$, validate the assignment of O_4 to the oxidation of the 17-electron radical $CpNi(PR_3)$.

However, the size of O_4, even when generated from the reduction of $Cp(PR_3)NiCl$, is sometimes much smaller than expected for a quantitative oxidation of $CpNi(PR_3)$. In those systems where O_4 is small, the reversible oxidation wave O_5 of nickelocene is clearly identified. Indeed, in the case of $Cp(PPh_3)NiCl$ in THF, wave O_4 is at least 10 times bigger than O_5 at 20 V s^{-1}, whereas at 0.5 V s^{-1}, O_5 overtakes O_4, see Figs. 4b and 4c. This demonstrates that the nickelocene that is oxidized at wave O_5 is not produced by the oxidation performed at O_4, i.e., does not result from the decomposition of the monophosphine cation, but rather illustrates the poor stability of the monophosphine radical itself [eqn. (4)].

$$Cp(PR_3)NiCl + e \rightarrow CpNi(PR_3) + Cl^- \quad \text{wave } R_1^* \qquad \text{(overall}^{15}\text{ eqn. 3)}$$

$$CpNi(PR_3) \rightarrow 1/2\ Cp_2Ni + ? \qquad (4)$$

$$CpNi(PR_3) - e \rightarrow CpNi(PR_3)^+ \rightarrow ? \quad \text{wave } O_4 \qquad (5)$$

$$Cp_2Ni - e \rightleftharpoons Cp_2Ni^+ \quad \text{wave } O_5 \qquad (6)$$

At the same potential scan rate, waves O_4 are bigger for PBu_3 than PPh_3 in a given solvent, and bigger in THF than in acetonitrile for a given phosphine: this is indicative of the factors which control the decomposition of $CpNi(PR_3)$. The more strongly ligated tributylphosphine stabilises the 17-electron intermediate and so does the less coordinating solvent THF; this suggests that the decomposition pathway could involve a solvent-assisted

decoordination of the last phosphine [eqn. (7)] followed by a transfer of a cyclopentadienyl ligand [eqn. (8)].

$$CpNi(PR_3) + n\ Solv. \rightarrow CpNi(Solv.)_n + PR_3 \quad (7)$$

$$CpNi(Solv.)_n + CpNi(PR_3) \rightarrow Cp_2Ni + Ni(PR_3)(Solv.)_n \quad (8)$$

Nickelocene is formed in a quantitative yield during the electrolysis of $Cp(PPh_3)NiCl$ in acetonitrile at the potential of formation of $CpNi(PR_3)$; no other isolable compound corresponding to the remaining nickel (50%) could be identified by cyclic voltammetry or spectroscopy in agreement with the above formulation of $Ni(PR_3)(Solv.)_n$, a species which is expected to undergo clustering. The scheme above [eqns. (3), (7), (8)] implies an overall 1F reduction corresponding to the monoelectronic reduction of $Cp(PR_3)NiCl$ to $CpNi(PR_3)$ since the two equations (7) and (8) do not involve any electron transfer. However, the experimental electron consumption was clearly lower than 1 in electrolysis; this unexpected result may be due to a competitive inner-sphere type reduction of $Cp(PPh_3)NiCl$ by the poorly ligated nickel(0) species or clusters formed from it, which would also generate $CpNi(PR_3)$ and a non-electroactive nickel halide.[17]

Electrogeneration, stability and quenching of the 18-electron nickel(0) anion. The one-electron reduction that takes place at wave R_2 [eqn. (9)] generates the 18-electron nickelate; this nickel(0) anion evolves in the medium on the one-second timescale, as shown by the poor chemical reversibility of R_2. The complete irreversibility of this wave in the presence of hydroquinone (Fig. 3a) acting as a proton donor corresponds to the formation of the nickel hydride.

$$CpNi(PPh_3) + e \rightarrow CpNi(PPh_3)^- \quad (9)$$

$$CpNi(PPh_3)^- + AH \rightarrow CpNi(PPh_3)H + A^-$$

The electrolysis of $Cp(PPh_3)NiCl$ at the potential of wave R_2, gave rigorously the same results as the electrolysis previously described and performed at the potential of R_1: the same low electron consumption and the same quantitative formation of nickelocene. Even if a decomposition of the anionic species also leading to nickelocene cannot be ruled out, a most likely hypothesis is a fast homogeneous electron transfer reaction [eqn. (10)] between this anion and the starting chloride, responsible for the regeneration of the 17-electron radical in the solution and subsequent identical fate. The potentials given in Table 2 ($\Delta E^p > 0.6$ V) strongly suggest that the electron transfer considered here is thermodynamically favourable, even if a definitive conclusion cannot be drawn from irreversible peak potentials.

$$CpNi(PPh_3)^- + Cp(PPh_3)NiCl \rightarrow 2\ CpNi(PPh_3) + Cl^- \quad (10)$$

The nickelate could, alternatively, be quenched in the diffusion layer by a powerful non-reducible electrophile [eqn. (11)], leading to the mixed bimetallic complex $Cp(PPh_3)NiSnPh_3$ whose reversible reduction is visible at a slightly lower potential (Fig. 3b).

$$CpNi(PPh_3)^- + R_3SnCl \rightarrow Cp(PPh_3)NiSnR_3 \quad (11)$$

$$Cp(PPh_3)NiSnR_3 + e \rightleftharpoons Cp(PPh_3)NiSnR_3^-$$

The very negative reduction potential of triphenyltin chloride ($E^p = -2.48$ V) excludes the possibility of any alternative pathway to the mixed bimetallic complex $Cp(PPh_3)NiSnPh_3$ observed in cyclic voltammetry at -1.7 V and electrolysis, which would involve the initial reduction of Ph_3SnCl, either at the electrode or by $CpNi(PPh_3)^-$, followed by the reaction of the thus-formed Ph_3Sn^- with the starting nickel chloride.[16] This is all the more true for the tributyltin analogue.

Reaction (11) has to be fast to give rise to a voltammogram such as the one depicted in Fig. 3b since the time elapsed between the formation of the nickelate (wave R_2) and the analysis of the product is very short (200 mV at 0.5 V s^{-1} corresponds to less than 0.5 s). In this respect, it may be surprising that the yields of $Cp(PPh_3)NiSnR_3$ are rather modest in preparative experiments, even when working with an excess of electrophile. In fact, two points should be considered: (*i*) a possible effect of the solvent on the competition between the two electrophiles, R_3SnCl leading to the mixed bimetallic compound [eqn. (11)] and $Cp(PPh_3)NiCl$ leading to nickelocene [eqns. (10) and (4)], and (*ii*) the unavoidable reduction of part of the product at the electrolysis potential due to the small difference between the potential of nickelate formation and the potential of $Cp(PPh_3)NiSnPPh_3$ reduction. The significant increase of the number of faradays when tributyl- or triphenyltin chloride is present is then easily understood since the reaction of $CpNi(PPh_3)^-$ with $Cp(PPh_3)NiCl$ formally requires 1F, and, in fact, less due to follow-up reactions as discussed above, whereas the quenching of the same anion by the tin electrophiles consumes 2F and possibly more if the mixed bimetallic product is partially reduced.

Mononuclear vs *dinuclear nickel(I) species* In the whole discussion above, it is considered that the 17-electron radical is stable enough to survive, during the time elapsed in cyclic voltammetry in THF, between its formation at wave R_1 or R_1* and its reduction [eqn. (9)] at wave R_2 or oxidation [eqn. (5)] at wave O_4. In acetonitrile, or on a longer timescale it is readily transformed into nickelocene. This is the simplest scheme that accounts for the experimental observations. However, it is impossible, on the basis of these data, to exclude the possibility of an equilibrium between the radical and its dimer or even a fast irreversible dimerization of this 17-electron species. Indeed, the electrochemical behaviour would then be the same if the dimer were reduced at wave R_2 to form an 18-electron anion[18] or were oxidised at wave O_4. The same is true for the product of the reaction (11) between $Cp(PPh_3)NiCl$ and $CpNi(PPh_3)^-$.

Since there is no means of determining the difference

from the electrochemical data, we favoured the involvement of the 17-electron mononuclear species based on a chemical point of view. Indeed, dimeric complexes of nickel(I) are uncommon and seem to be restricted[19] to a set of cyclopentadienylnickel carbonyl dimers $[CpNi(CO)]_2$, which benefit from the stabilising presence of two bridging CO ligands. The strong π acceptor character of CO may be of importance but the most important point is certainly the cohesion brought by the bridges in addition to the metal–metal bond. In a related way, more electron-donating bridging ligands allow the formation of symmetrical Ni^{II} dimers such as $[CpNi(\mu\text{-}SR)]_2$ or $[CpNi(\mu\text{-}PR_2)]_2$ without a nickel–nickel bond. A fast dimerisation of the 17-electron $CpNi(PR_3)$ where no bridged structure can be formed therefore seems disfavoured compared with the ligand-scrambling reaction which eventually leads to nickelocene.

Conclusions

The electrochemical reduction of cyclopentadienylnickel phosphine complexes leads to nickel(I) species: the 19-electron bis-phosphine radical $CpNi(PR_3)_2$ generated from the corresponding cation readily loses one phosphine ligand via a reversible process that can be dynamically displaced during cyclic voltammetry experiments. The so-formed 17-electron compound, which is also directly obtained by the monoelectronic reduction of $Cp(PR_3)NiCl$, is rather unstable and undergoes, in the 0.01–1 s range, a chemical disproportionation reaction that leads to nickelocene and a reducing poorly ligated nickel species. Further reduction of this 17-electron radical provides an electron-rich nickelate which is very similar to the known[20] anion $CpNi(CO)^-$, although far less stable as expected from the replacement of the CO ligand by a phosphine. Nevertheless, it was possible to quench and characterise this new nickelate by its stannylation, as had been done previously for the stable carbonyl homologue.[21]

Experimental

Chemicals. THF was purified by distillation from sodium–benzophenone under argon, and acetonitrile was distilled over calcium hydride; both solvents were thoroughly degassed prior to use. Nickelocene (Fluka), Triphenylphosphine (Aldrich), tributylphosphine (Janssen) and triphenyltin chloride (Ventron) were stored under argon and used without further purification.

The starting nickel complexes were prepared according to previously published procedures: $Cp(PPh_3)NiCl$,[22] $Cp(PBu_3)NiCl$,[22] $[CpNi(PPh_3)_2^+, BF_4^-]$,[23] $[CpNi(PBu_3)_2^+, BF_4^-]$,[24] $Cp(PPh_3)NiSnPh_3$.[16] All the chemical and electrochemical experiments were run under argon. $n\text{-}Bu_4NBF_4$ was used as the supporting electrolyte; it was obtained from $n\text{-}Bu_4N \cdot HSO_4$ and $NaBF_4$, recrystallized from ethyl acetate–hexane and dried at 60 °C under vacuum.

Cyclic voltammetry. CV experiments were performed in an air-tight three-electrode cell connected to a vacuum line. The reference electrode was SCE (Tacussel) separated from the solution by a bridge compartment filled with the same solvent supporting electrolyte solution as that used in the cell. The counter electrode was a platinum spiral wire with ca. 1 cm^2 apparent surface area. The working electrodes were disks obtained from cross-sections of gold wires (diameters 25–500 μm). A EG&G PAR-175 signal generator was used; the potentiostat was home-made,[25] with a positive feedback loop for ohmic drop compensation. The currents and potentials were recorded on a Nicolet 310 oscilloscope.

Preparative-scale electrolyses. These were performed in a separated H cell; the counter-electrode (anode) was a platinum grid with a ca. 7 cm^2 apparent surface, and the cathode was a gold grid of the same size. A Tacussel PJT 35-2 potentiostat and a Tacussel IG 5LN integrator monitored the electrolyses which were performed on a 100 mg scale in a 30 ml cathodic compartment. The reduction of $Cp(PPh_3)NiCl$ and the formation of nickelocene as a function of the number of faradays passed through were followed by *in-situ* cyclic voltammetry at a microelectrode set in the cathodic compartment, the gold grid then being used as a counter-electrode.

Acknowledgements. This work was supported by the CNRS (UMR 8640) and the *Ecole Normale Supérieure*, Paris. The French Ministry of Research is gratefully acknowledged for a Ph.D. grant to O.B.

References

1. Geiger, W. E. *Acc. Chem. Res. 28* (1995) 351.
2. Geiger, W. E. *Prog. Inorg. Chem. 33* (1985) 275.
3. Pombeiro, A. J. L. and McCleverty, J., Eds. In: *Molecular Electrochemistry in Inorganic, Bioinorganic and Organometallic Compounds*, NATO ASI Series, Kluwer, Dordrecht 1993.
4. Chanon, M., Julliard, M. and Poite, J. C., Eds., *Paramagnetic Organometallic Species in Activation, Selectivity and Catalysis*, Kluwer, Dordrecht 1989.
5. Trogler, W. C., Ed. In: 'Organometallic Radical Processes', *J. Organomet. Chem. Library 22*, Elsevier, Amsterdam 1990.
6. Astruc. D., In: *Electron Transfer and Radical Processes in Transition-metal Chemistry*, VCH, New York 1995.
7. Jolly, P. W. and Wilke, G. In: *The Organic Chemistry of Nickel: Organometallic Chemistry. A Series of Monographs.* Maitlis, P. M., Stone, F. G. A. and West, R. Eds. Academic Press, New York 1974, Ch. IV, pp. 215–234.
8. Nag, K. and Chakravorty, A. *Coord. Chem. Rev. 33* (1980) 87.
9. Koelle, U. and Werner, H. *J. Organomet. Chem. 221* (1981) 367.
10. Barefield, E. K., Krost, D. A., Edwards, D. S., Van Derveer, D. G., Trytko, R. L. and O'Rear, S. P. *J. Am. Chem. Soc. 103* (1981) 6219.
11. Bermudez, G. and Pletcher, D. *J. Organomet. Chem. 231* (1982) 173.

12. Amatore, C., Azzabi, M., Calas, P., Jutand, A., Lefrou, C. and Rollin, Y. *J. Electroanal. Chem. 288* (1990) 45.
13. The origin of this prewave was established on the basis of its decrease in size with increasing scan rate, as expected for a CE mechanism[14] and complementary CV experiments where either $AgBF_4$ or $NBu_4^+ Cl^-$ were purposely added to displace the equilibrium between $Cp(PR_3)NiCl + ACN$ and $Cp(PR_3)Ni(ACN)^+ + Cl^-$.
14. Bard, A. J. and Faulkner, L. In: *Electrochemical Methods,* Wiley, New York 1980.
15. The reduction of $Cp(PR_3)NiCl$ in THF was found to be controlled by heterogeneous electron transfer, as shown by the slopes[14] of the plot of E^p vs. log v (potential scan rate): 70 and 50 mV per decade, respectively, for R = Bu and R = PPh_3. These values may suggest a concerted cleavage of the anion radical rather than an EC mechanism; however, no investigation was undertaken to answer this question.
16. Thomson, J. and Baird, M. C. *Inorg. Chim. Acta* (1973) 105.
17. Such a reaction would lead to $NiCl_2(PPh_3)_2$ or anything equivalent to this stoichiometry, and would indeed be the reverse of the preparation of $Cp(PPh_3)NiCl$ from nickelocene;[22] the electrochemistry of $NiCl_2(PPh_3)_2$ has been investigated: Troupel, M., Rollin, Y., Perichon, J. and Fauvarque, J. F. *New J. Chem. 4* (1981) 621 and references therein.
18. For a related reduction in the stable cyclopentadienylnickel carbonyl family, see Dessy, R. E., Pohl, R. L. and King, R. B. *J. Am. Chem. Soc. 88* (1966) 5121.
19. Jolly, P. W. In: Wilkinson, G., Stone, F. G. A. and Abel, E. W., Eds., *Comprehensive Organometallic Chemistry,* Pergamon, Oxford 1982, Vol. 6, Chaps. 37–38.
20. Schroll, G. E. U.S. Pat. 3,054,815 (1962); see also Barnett, K. W. *J. Chem. Educ. 51*, (1974) 423.
21. Ellis, J. E., Faltynek, R. A. and Hentges, S. G. *J. Organomet. Chem. 120* (1976) 389.
22. Gompper, R. and Bartmann, E. *Liebigs Ann. Chem.* (1980) 229.
23. Treichel, P. M. and Shubkin, R. L. *Inorg. Chim. Acta* (1968) 485.
24. Sato, M., Sato, F. and Yoshida, T. *J. Organomet. Chem. 31* (1971) 415.
25. Amatore, C., Lefrou, C. and Pflüger, F. *J. Electroanal. Chem. 43* (1989) 270.

Received December 21, 1998.